

A CFD Analysis of Winglet Configuration to study its effects on Aircraft Performance

Dharmendra A Ponnaswami¹, Akash Mishra², Hitesh Kumar M³, Nasrin Ansari⁴, Prathamesh Patil⁵

¹Assistant Professor, Department of Aeronautical Engineering, DSCE, Bengaluru, 560078.

^{2,3,4,5}Student, Department of Aeronautical Engineering, DSCE, Bengaluru, 560078.

Abstract - Winglets are lifting surfaces fixed at the tip of wings for decreasing the trailing vortex drag and in to increase the aerodynamic efficiency of the wing. The project intends to show the effect of winglets on Airplane wings by comparing both wings with and without winglets. It studies the difference by Analysing the coefficient of drag on the wings with the use of winglets at different Cant angles to different Angle of Attack, to find the best Cant angle that reduces Drag to a minimum level so that the Aerodynamic Performance can be increased (Increase in the lift at the same fuel consumption). Blended winglet configuration is designed in SOLIDWORKS and Analysed using ANSYS FLUENT software.

Key Words: Aerodynamic Performance, Cant Angle, Winglet, Angle of Attack (AOA).

1. INTRODUCTION

The Aerodynamic force is one of a significant force that keeps an aircraft afloat in the air. This force acts over on an aircraft and depends significantly on aircraft design and relative parameters. Thus, the need to curb the drag and increase the overall lift of an aircraft has been a topic of interest for many researchers in the field of aerodynamics.

Drag such as at the wing tip leads to the formation of wingtip vortices. Vortices are defined as a region in a fluid where the flow revolves around an axis line that can either be straight or curved. Thus, during the evolution of aircraft design, the necessity to reduce aircraft drag led to the development of what we today know as winglets.

Winglets are engineered designed accessory attached at the end of the wing to reduce the drag of the aircraft acting at winglets and thus increase the overall lift of the aircraft. The winglet design is adopted by observing the bird's flying pattern and the way these birds tend to flap and move their wings in the sky.



Fig-1: Vortex formation over a wing. (Courtesy: Internet)

Fig-1 represents how a winglet attachment to the wing leads to a change in the flow pattern of air around the wing. Winglets increase the aspect ratio of a wing by not adding additional

structural stress on and aircraft. The performance of an aircraft significantly changes when a winglet is attached to the wing to that of which compared to an aircraft with only plane wings. The need to study the variable cant angle of a wing placed at a different angle of attack and the change of overall performance by changing these parameters can help the future designers to design a flexible configuration which will lead to an increase in performance of aircraft without adding additional load on aircraft structure.

2. METHODOLOGY

2.1. DESIGN OF AEROFOIL

The NACA 4 series airfoil coordinate generator is used to retrieve data points to plot the airfoil coordinates into the software like SOLIDWORKS, CATIA V5, AUTOCAD, etc. These Designing software's are used to generate the aircraft wing for our considered configurations.

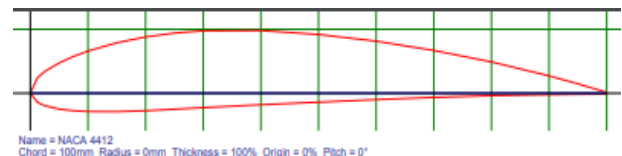


Fig-2: Airfoil Coordinates of NACA 4412. (Courtesy: NACA)

Fig-2 is NACA 4412 airfoil coordinate, this is imported into designing tool and then plane wing and wing with winglet configuration is designed as per the specifications.

2.2. DESIGN OF PLANE WING CONFIGURATION.

The design of a plane wing configuration is carried out using SOLIDWORKS. Table-1 represents the specification used to design the wing configuration while Fig-3 is an isometric view of the final plane wing configuration design.

Table-1: Specification of plane wing configuration.

SI No.	Description	Dimension
01	Airfoil Type	NACA 4412
02	Wing Type	Swept Back
03	Sweep Angle	19.03°
04	Wingspan	22 cm
05	Taper Ratio	0.27
06	Aspect Ratio	3.7
07	Wing Area	130.8 cm ²

08	Maximum Chord	9.4 cm
09	Minimum Chord	2.5cm

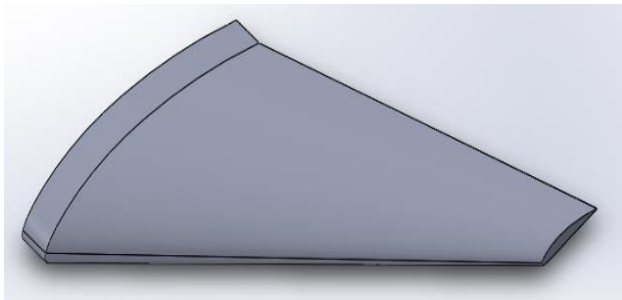


Fig-3: Isometric view of the wing

2.3. DESIGN OF WING WITH WINGLET CONFIGURATION

The design of the wing with winglet configuration is carried out using SOLIDWORKS. Table-2 represents the specification used to design the winglet configuration while Fig-4 is an isometric view of the final wing with winglet configuration design. Similarly, another wing with winglet configuration at different Cant angle is designed for analysis and thus one such design is shown in Fig-4.

Table-2: Specifications of Winglet.

SI No.	Description	Dimension
01	Winglet Type	Blended Winglet
02	Winglet Span	2 cm
03	Winglet Height (30° & 90°)	1 cm & 1.5 cm
04	Winglet Area	5 cm ²
05	Winglet Sweep Angle from the wingtip	47.73°
06	Winglet Taper Ratio	0.12
07	Maximum Chord	2.5 cm
08	Minimum Chord	0.3 cm

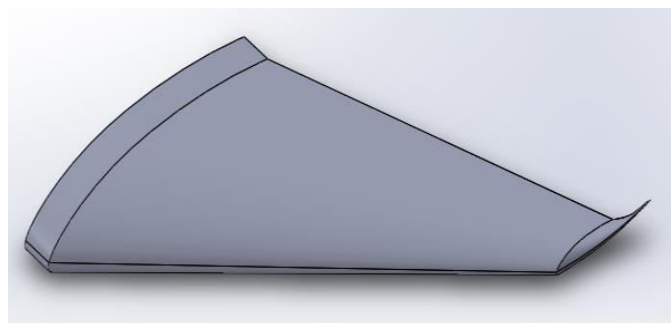


Fig-4: Isometric view of a wing with winglet configuration at 30° Cant angle.

2.4. DOMAIN MODELLING

The designed model of the wing and wing with winglet configuration is been imported into ANSYS FLUENT (Geometry). Fig-5 is the specification used to design the model

around the configurations of the wing and winglet used for analysis.

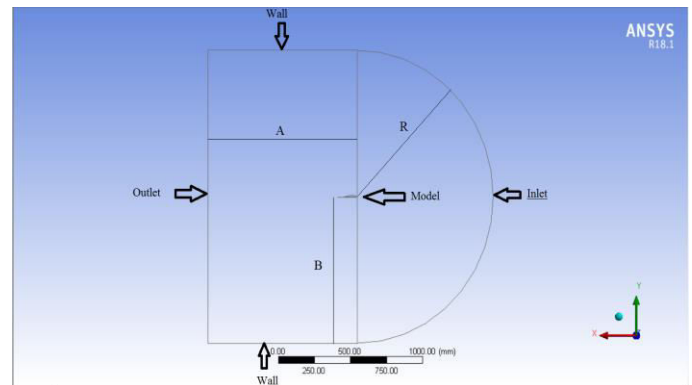


Fig-5: Side view of the designed Domain.

2.5. MESHING

The Meshing is performed using global mesh attributes for the considered cases that are a plane wing, a wing with winglet configuration at 30°, 45°, and 60° Cant angle. Unstructured tetrahedral elements are employed with inflation being carried over the wing and wing with winglet configuration keeping element size for inflation as 0.05cm and 8 layers respectively for all the cases.

Table-3: Meshing Details

	Without Winglet	With Winglet
No of Elements	24,55,774	24,86,805
No of Nodes	7,98,343	8,05,056

Table-3 signifies the number of mesh elements details and nodes respectively. Fig-6, Fig-7, and Fig--8 are the meshed views of a wing with winglet configuration at 30° Cant angle configuration, this similar approach is used for meshing all other cases.

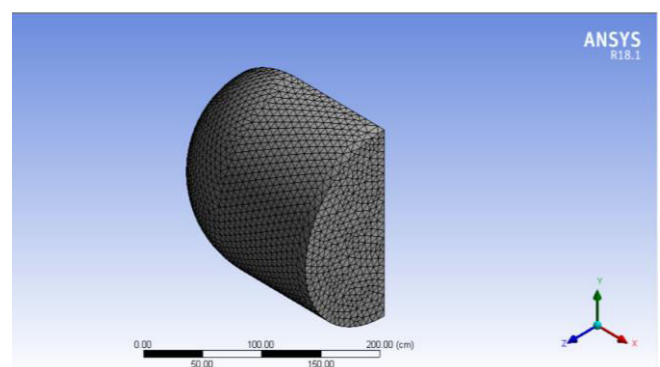


Fig-6: Isometric view of the meshed domain.

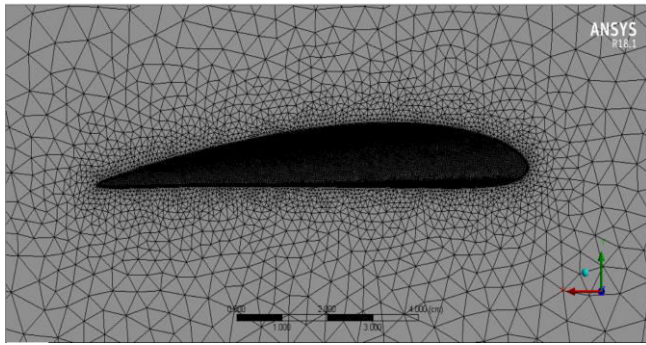


Fig-7: Magnified right view of Mesh.

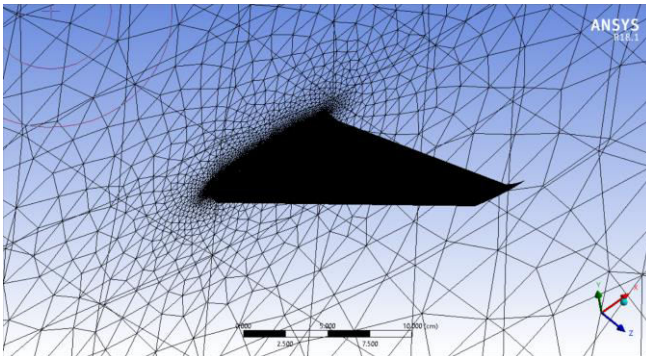


Fig-8: Magnified view of meshed Wing with Winglet at 30° Cant angle.

2.5 ANALYSIS SETUP

The Numerical calculations have been carried out through ANSYS FLUENT with the help of a 3-D steady-state pressure-based $K-\omega$ turbulence model using ANSYS FLUENT. The Inlet velocity is considered to be 50 m/s, while the convergence factor is set as 0.00001. At the solid wall(s), the no-slip boundary condition is considered. An Ideal gas has been considered under the setup to be as the working fluid. Table-4 represents the Boundary conditions used in ANSYS FLUENT Setup.

Table-4: Boundary Conditions.

Sl. No	Boundary Condition	
01	Model	$K-\omega$ Turbulence Model
02	Fluid	Ideal gas
03	Flow Condition	Steady-state
04	Inlet	Velocity Inlet=50m/s
05	Outlet	Pressure Outlet
06	Symmetry	Symmetry
07	Farfield	Wall
08	Convergence factor	0.00001
09	Solver	Pressure Based

3. RESULTS AND DISCUSSION

The Numerical calculations after setting up the analysis setup were carried out in ANSYS FLUENT solver, where the hybrid initialization was initiated after using the boundary conditions as

mentioned in Sec-2.5. CFD post-processing tool plotted the various contours of pressure and velocity for all the considered cases.

The C_L and C_D values were retrieved from the analysis carried out and were later tabulated. The respective plots of these values were drawn using Microsoft Excel.

Table-5 shows tabular information of the analysis results obtained. As discussed in the previous paragraph these values are obtained in the ANSYS FLUENT solver for all the considered wing and wing with winglet configuration at different Cant angle along with that at a different angle of attack.

Table-5: Generated values of C_L and C_D for considered cases.

AOA/Cant angle		Normal wing	Wing with 30° winglet	Wing with 45° winglet	Wing with 60° winglet
-2°	C_L	-0.0912	-0.1103	0.0588	0.0561
	C_D	0.0304	0.0306	0.0324	0.0324
0°	C_L	0.0751	0.0818	0.1234	0.1235
	C_D	0.021	0.023	0.0314	0.0219
+2°	C_L	0.2035	0.205	0.1991	0.1966
	C_D	0.0305	0.0198	0.0389	0.0382
+4°	C_L	0.3036	0.3621	0.374	0.3134
	C_D	0.0611	0.0423	0.0441	0.0402
+6°	C_L	0.3882	0.4738	0.4762	0.4762
	C_D	0.0746	0.0536	0.054	0.0512

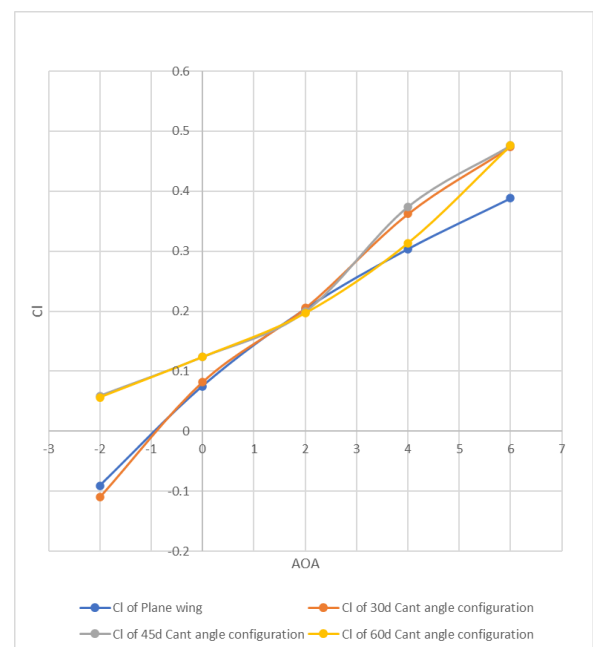


Fig-9: C_L versus AOA Plot

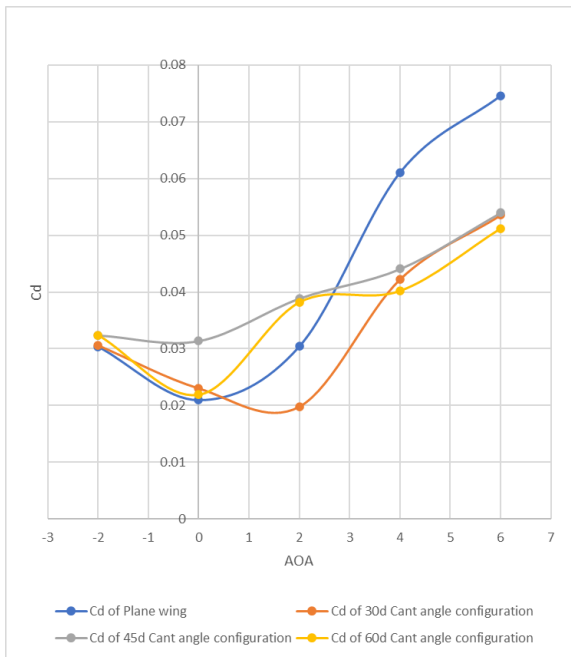


Fig-10: C_D versus AOA Plot

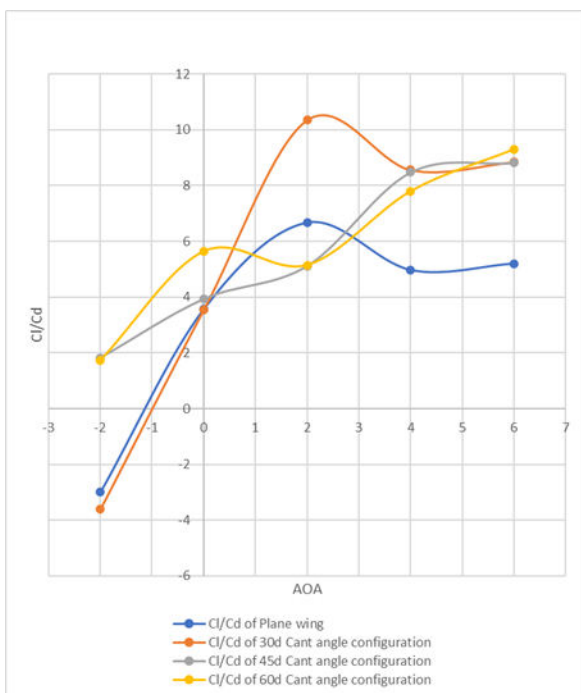


Fig-11: C_L/C_D versus AOA Plot

Fig-9, Fig-10, and Fig-11 are the plots of C_L , C_D and C_L/C_D with respect to the angle of attack at different Cant angle configuration. These plots are plotted using the Table-5.

In Fig-9, if one may notice that the lift coefficient is high for wing with winglet configuration at -2 angle of attack for 45° Cant angle configuration. As the angle of attack was increased, the lift coefficient for all the cases also increased, at +6 angle of attack the least lift coefficient is achieved for 60° Cant angle configuration.

In Fig-10, we see that the drag coefficient reduces initially with an increase in the angle of attack and later it significantly increases as the angle of attack is increased. The minimum drag coefficient among all the cases is achieved for 30° Cant angle configuration at +2 angle of attack and likewise, the maximum

drag is observed for the plane wing configuration at +6 angle of attack.

In Fig-11, we observe that initially, the C_L/C_D value increases with an increase in the angle of attack. The maximum C_L/C_D value is obtained for 30° Cant angle configuration at +2 angle of attack and the least values of C_L/C_D are observed for the same configuration at -2 angle of attack. Similarly, C_L/C_D value for 45° Cant angle configuration at 0 Angle of attack is larger than that of other cases. At 6 angle of attack, the value of C_L/C_D for 60° Cant angle configuration is better than other configurations.

The isometric view of Pressure and Velocity contour for the maximum value of C_L/C_D , C_L and C_D at a different angle of attacks referring from Table-5 and Fig-11 is presented in the below figures. The other cases contour is omitted out of this paper as the author(s) had seen a similar variation of the pressure and velocity along with the considered configurations.

Fig-12, Fig-14, Fig-16, Fig-18, and Fig-20 represent the Pressure Contour of the wing with winglet configuration yielding the best C_L/C_D value during CFD analysis.

Fig-13, Fig-15, Fig-17, Fig-19, and Fig-21 represent the Velocity Contour of the wing with winglet configuration yielding the best C_L/C_D value during CFD analysis.

As we see in Fig-12, the pressure variation from the root to tip gets concentrated as it moves away from the wing root on the upper surface of the configuration. Also, pressure variation from leading edge as it moves towards trailing edge reduces and later recovers causing a low-pressure region. At the lower surface of the configuration, the pressure is significantly high.

Thus from the previous paragraph, we can see that this similar pattern is formed in all the pressure contours presented and considered as in Table-5. This is seen in the pressure contours for the cases as in Fig-14, Fig-16, Fig-18, and Fig-20.

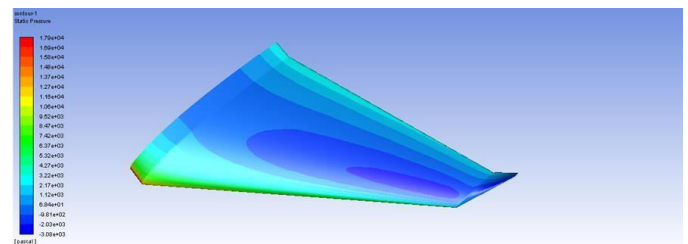


Fig-12: Isometric Pressure contour view of 30° Cant angle wing with winglet configuration at +2 AOA.

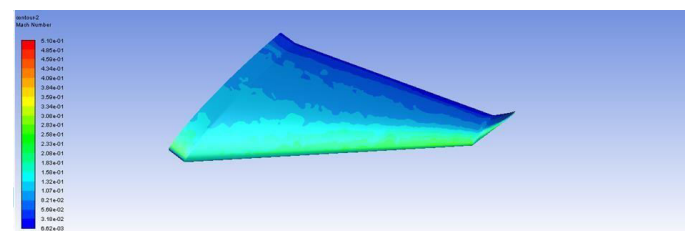


Fig-13: Isometric Velocity contour view of 30° Cant angle wing with winglet configuration at +2 AOA.

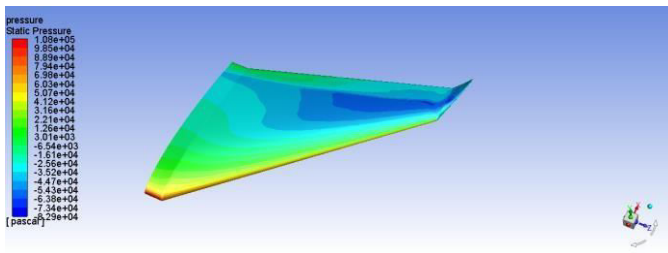


Fig-14: Isometric Pressure contour view of 30° Cant angle wing with winglet configuration at +4 AOA.

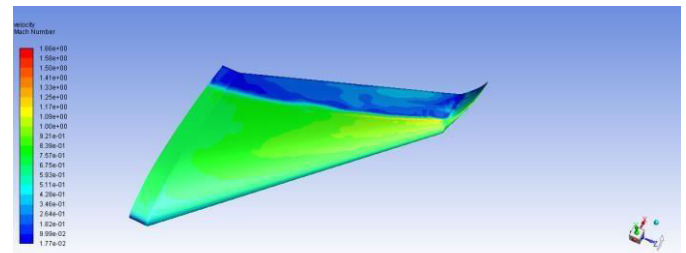


Fig-19: Isometric Velocity contour view of 60° Cant angle wing with winglet configuration at 0 AOA.

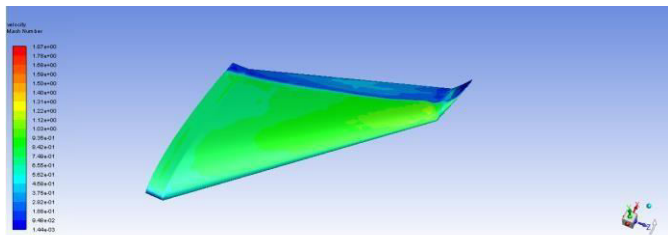


Fig-15: Isometric Velocity contour view of 30° Cant angle wing with winglet configuration at +4 AOA.

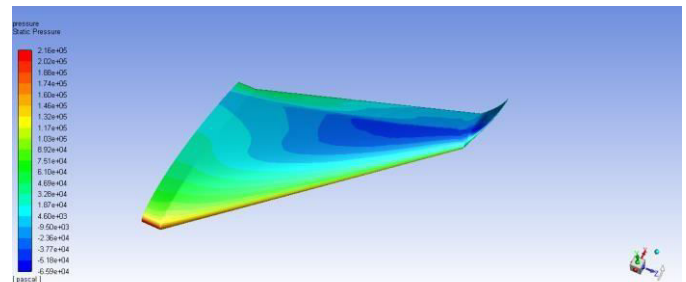


Fig-20: Isometric Pressure contour view of 60° Cant angle wing with winglet configuration at +6 AOA.

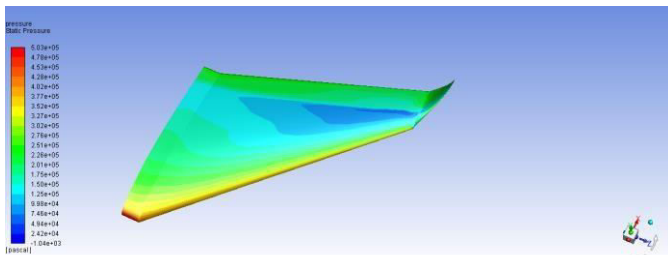


Fig-16: Isometric Pressure contour view of 45° Cant angle wing with winglet configuration at -2 AOA.

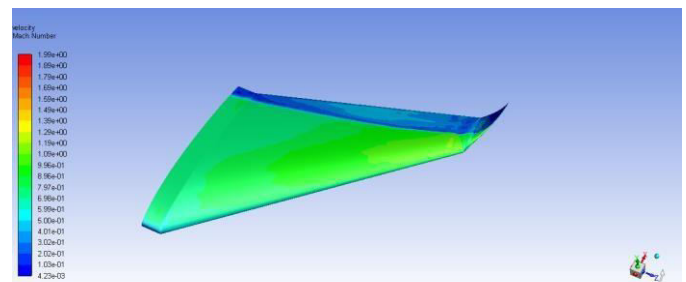


Fig-21: Isometric Velocity contour view of 60° Cant angle wing with winglet configuration at +6 AOA.

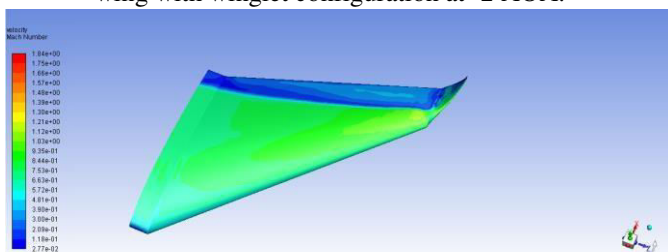


Fig-17: Isometric Velocity contour view of 45° Cant angle wing with winglet configuration at -2 AOA.

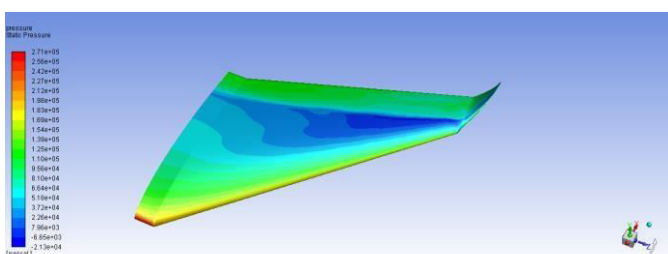


Fig-18: Isometric Pressure contour view of 60° Cant angle wing with winglet configuration at 0 AOA.

As we see in Fig-13, the velocity variation from leading edge as it moves towards trailing edge reduces for the upper surface of the wing while at the lower surface of the configuration the velocity is significantly low as it moves from leading edge to trailing edge.

Thus, from the previous paragraph, we can see that this similar pattern is formed in all the velocity contours presented and considered as in Table-5. This can be seen for the pressure contours cases as in Fig-15, Fig-17, Fig-19, and Fig-21.

4. CONCLUSION

In this paper, the above plots, tables, and color contours signify the best results obtained during analysis and the calculation of C_L/C_D . Thus overall, those fore drawn figures are the representation of best results. Thus, we conclude by stressing that the configuration of a wing with winglet yields best C_L/C_D than that of a plane wing, Also, we highlight how the overall lift and drag with respect to the angle of attack and Cant angle can be the important parameter and can be considered for the overall increase in aircrafts performance, one such being an increase in the lift without increasing the wingspan while also decreasing at the same time the overall drag by using the winglets, we also see that this reduces the whole weight of the aircraft and there are not many changes on its structural design. This gives us the scope to design such a wing configuration that can use variable winglet technology and change accordingly when required

during the flight of an aircraft. The overall performance with the introduction of the winglet leads to a decrease in fuel consumption of the engine as it doesn't have to produce additional thrust to overcome the drag. Thus, further analysis for several variable winglet configurations on different types of winglet designs can be taken up and a comparative study can be performed.

ACKNOWLEDGMENT

We appreciate NACA airfoil tools web source for many data coordinates values and plots embedded in it.

REFERENCES

1. Dinesh Myilsamy, Yokesh Thirumalai and Premkumar P.S, "Performance Investigation of an Aircraft Wing at Various Cant Angles of Winglets using CFD Simulation", India Altair Technology Conference, 2015.
2. Naveen Balakrishnan and Ganesh, "Design Modification of Winglet Concept to Increase Aircraft's Efficiency", IJESMR, 2015.
3. Ali Murtaza, Dr. Khalid Parvez, Hanzala Shahid, and Yasir Mehmood, "Design and Computational Fluid Dynamic Analysis of Spiroid Winglet to Study Its Effects on Aircraft Performance", IRJET, 2017.
4. Saravanan Rajendran, "Design of Parametric Winglets and Wingtip devices - A conceptual Design Approach", Linkoping University, 2012.
5. Alekhya N, N Prabhu Kishore, and Sahithi Ravi, "Performance Analysis of Winglet at Different Angle of Attack", IRJET, Volume 3 issue:9, 2016.
6. T Ravikumar Reddy, Prajwal Kumar M Patil, and G Sudarshan Reddy, "Modeling and CFD Analysis of Flow Over Aircraft Split Winglet and Blended Winglet", IJASRE, 2018.
7. Mohammed Salahuddin, Mohd Obaid-ur-Rahman, Shaik Jaleel, "A Report on Numerical Investigation of Wings: with and without Winglet", IJRAME, Volume 1 Issue:1, 2013.
8. Nicolas El Haddad, "Aerodynamic and Structural Design of a Winglet for Enhanced Performance of a Business Jet", Embry-Riddle Aeronautical University Scholarly Commons, 5-2015.
9. Eastman N. Jacobs, Kenneth E. Ward, and Robert M. Pinkerton. NACA Report No: 460 "The Characteristics of 78 related Airfoil Sections from Tests in the Variable-Density Wind Tunnel", NACA, 1935.
10. John D. Anderson, Jr., "Fundamentals of aerodynamics", third edition., chapter 4, pp.280,2001.

BIOGRAPHIES



Dharmendra A Ponnaswami¹, Assistant Professor at Dayananda Sagar College of Engineering. His qualifications are Bachelor of Engineering in Mechanical Engineering and Master of Technology in Aeronautical Engineering. He has been the technical support and faculty coordinator member of the Institute of Aeronautics, Astronautics and Aviation (IAAA) since 2017 and also a professional member of the Institute of Engineering Research and Publication (IFERP) since 17th

Dec 2019. He has presented many papers in various journals and conferences and has also conducted workshops in this domain.



Akash Mishra² is a UG student of the aeronautical department at DSCE and currently pursuing his final year. He has a keen interest in the field of aircraft materials.



Hitesh Kumar M³ is a UG student of the aeronautical department at DSCE and currently pursuing his final year. He has a keen interest in the field of structures and is currently placed in Quest global PVT Ltd.



Nasrin Ansari³ is a UG student of the aeronautical department at DSCE and currently pursuing her final year. She has a keen interest in the field of aircraft engines and is currently placed in Capgemini.



Pratamesh Patil⁴ is a UG student of the aeronautical department at DSCE and currently pursuing his final year. He has a keen interest in the field of Product Design.